Available online at www.sciencedirect.com

SciVerse ScienceDirect

Ceramics International 38 (2012) 4845–4851

CERAMICS INTERNATIONAL

www.elsevier.com/locate/ceramint

Effect of $Ba_{0.85}Ca_{0.15}Ti_{0.90}Zr_{0.10}O_3$ content on the microstructure and electrical properties of $Bi_{0.51}(Na_{0.82}K_{0.18})_{0.50}TiO_3$ ceramics

Sha Qiao, Jiagang Wu *, Bo Wu, Binyu Zhang, Dingquan Xiao, Jianguo Zhu

Department of Materials Science, Sichuan University, 610064, PR China

Received 6 February 2012; received in revised form 23 February 2012; accepted 23 February 2012
Available online 3 March 2012

Abstract

$(1-x)Bi_{0.51}(Na_{0.82}K_{0.18})_{0.50}TiO_3$–$xBa_{0.85}Ca_{0.15}Ti_{0.90}Zr_{0.10}O_3$ [$(1-x)$BNKT–xBCTZ] ceramics were prepared by the conventional solid-state method, and the effect of BCTZ content on their microstructure and electrical properties was investigated. A stable solid solution with a pure perovskite phase is formed between BNKT and BCTZ, and these ceramics have a coexistence of rhombohedral and tetragonal phases in the range of $0 \leq x < 0.15$. Their T_m and T_d values are strongly independent on the BCTZ content. Moreover, the sintering temperature strongly affects the ferroelectric and piezoelectric properties of these ceramics with $x = 0.02$. These ceramics with $x = 0.02$ exhibit an optimum electrical behavior of $d_{33} \sim 205$, $k_p \sim 0.25$, $P_r \sim 31.8$ μC/cm^2, and $E_c \sim 19.1$ kV/cm together with a high T_d value of ~91 °C when sintered at 1180 °C and poled at an optimum condition. As a result, the $(1-x)$BNKT–xBCTZ ceramic is a promising candidate material for lead-free piezoelectric ceramics.

Keywords: C. Piezoelectric properties; Lead-free ceramics; $Bi_{0.51}(Na_{0.82}K_{0.18})_{0.50}TiO_3$; $Ba_{0.85}Ca_{0.15}Ti_{0.90}Zr_{0.10}O_3$; Microstructure

1. Introduction

Lead-based piezoelectric materials dominate the commercial market for electromechanical devices because of their superior piezoelectric and electromechanical properties [1]. However, the use of lead-based materials will be prohibited by the upcoming environmental regulations of the waste electrical and electronic equipment (WEEE) directive and the restriction of hazardous substances (RoHS) in Europe because of serious environmental pollution induced by their toxicity either during the manufacturing process evaporation of lead or after making the device. Therefore, it is expected that lead-free piezoelectric systems analogous to the $Pb(Zr,Ti)O_3$ (PZT) will be developed for replacing lead-based ceramics in various applications [2]. Lead-free bismuth perovskite ceramics have attracted much attention as one kind of promising alternatives for lead-based materials that have been widely used as piezoelectric sensors and electromechanical actuators [2–7].

Bismuth sodium titanate, ($Bi_{0.5}Na_{0.5}TiO_3$, BNT) is considered to be a potential lead-free piezoelectric ceramic candidate because of its large remnant polarization ($P_r \sim 38$ μC/cm^2) and high Curie temperature ($T_c \sim 320$ °C) [8]. However, a relatively low piezoelectric constant (d_{33}) and a low depolarization temperature (T_d) of these BNT ceramics hinder the practical application [8]. The barrier of a low d_{33} value in BNT could be resolved by forming solid solutions with other ferroelectrics with a view to improving its performance [9–11]. Among these BNT material systems, $(Bi_{1/2}K_{1/2})TiO_3$-modified BNT ceramics with a morphotropic phase boundary (MPB) of tetragonal and rhombohedral phases exhibit some excellent electrical properties, but their d_{33} values are still limited as compared to those of PZT ceramics. $Ba_{0.85}Ca_{0.15}Ti_{0.90}Zr_{0.10}O_3$ (BCTZ) ceramics have been recently given considerable attention because of their outstanding piezoelectric properties by constructing new phase boundary [12–14]. Therefore, it is highly expected that the introduction of BCTZ can further enhance the piezoelectric properties of $(Bi_{0.50}K_{0.50})TiO_3$-modified $(Bi_{0.50}Na_{0.50})TiO_3$ ceramics. Moreover, it is well known that the Bi element of BNT-based ceramics is easily evaporated when sintered at a high processing temperature, and an enhanced piezoelectric behavior could be induced by introducing the excessive Bi

* Corresponding author.
E-mail addresses: msewujg@scu.edu.cn, wujiagang0208@163.com (J. Wu).

0272-8842/$36.00
doi:10.1016/j.ceramint.2012.02.074

to BNT-based ceramics [15]. Therefore, it also becomes a tough issue to control the loss of the Bi volatile element in BNT-based ceramics by compensating the Bi content.

In the present work, $(1-x)Bi_{0.51}(Na_{0.82}K_{0.18})_{0.50}TiO_3$–$xBa_{0.85}Ca_{0.15}Ti_{0.90}Zr_{0.10}O_3$ [$(1-x)$BNKT–xBCTZ] ceramics with 1 mol% Bi excess were prepared by the conventional solid state method with a view of further improving the piezoelectric properties of BNT-based ceramics. Their microstructure and electrical properties were studied as a function of BCTZ content and different sintering temperatures, and the modification mechanism of BCTZ-doped BNT ceramics was also addressed. An enhanced d_{33} value of ~205 pC/N is induced for these ceramics by optimizing composition and experimental condition, for example, the BCTZ content, sintering temperature, and poling condition.

2. Experimental procedure

$(1-x)Bi_{0.51}(Na_{0.82}K_{0.18})_{0.50}TiO_3$–$xBa_{0.85}Ca_{0.15}Ti_{0.90}Zr_{0.10}O_3$ (x = 0, 0.02, 0.04, 0.08, 0.11, 0.15, 0.20, and 0.30) ceramics were prepared by the conventional solid state method. Raw materials used in this work were $BaCO_3$ (99%), $CaCO_3$ (99.0%), ZrO_2 (99.0%), K_2CO_3 (99.8%), Na_2CO_3 (99.8%), TiO_2 (99.99%), and Bi_2O_3 (99.9%). These powders were ball milled for 24 h with agate ball media and alcohol and then were dried by placing them in oven for 12 h. After calcination at ~850 °C for 6 h, these calcined powders were milled again for 12 h, and pressed into the disks of ~1.5 cm diameter and ~0.8 to 1.2 mm thickness under 10 MPa using a PVA as a binder. After burning off PVA, these pellets were sintered by using the crucible without any atmospheric powder at 1120–1200 °C for 2 h in air. Silver paste was sintered on both sides of samples at ~700 °C for 10 min to form the electrodes for their electrical measurements. These ceramics are poled in a ~15 °C silicone oil bath by applying the d_c electric field of 0~5.0 kV/mm for 20 min. All measurement of electrical properties of these ceramics is conducted after 24 h.

The phase structure of these sintered pellets was analyzed by using an X-ray diffraction (XRD) (DX1000, PR China). The density of these sintered pellets was determined by the Archimedes method. Surface morphologies of these ceramics were measured by the Field Emission Scanning electron microscopy (FE-SEM, Hitachi S-4800). The density of these sintered pellets was determined by the Archimedes method. The piezoelectric constant d_{33} of these ceramics was measured using a piezo-d_{33} meter (ZJ-3A, China). An impedance analyzer was employed to characterize the dielectric properties of these ceramics. The dielectric behavior as a function of temperature in these ceramics was obtained using an *LCR* meter (HP 4980, Agilent, USA). The polarization versus electric field (*P*–*E*) hysteresis loops of the ceramics were measured using a Radiant Precision Workstation (USA).

3. Results and discussion

Fig. 1(a) shows the XRD patterns of $(1-x)$BNKT–xBCTZ ceramics with different BCTZ contents, measured at room temperature. A stable solid solution is formed between BNKT and BCTZ, and no secondary phases were detected in all the ceramics in this work, confirming that the BCTZ diffuses into the BNKT lattice during sintering. Fig. 1(b) and (c) shows the expanded XRD patterns of these ceramics with different BCTZ contents. Their XRD peak positions are shifted to a lower angle with increasing BCTZ content, indicating an expansion of the unit cell volume because of the part substitution of Ba^{2+}/Ca^{2+}($r_{Ca^{2+}}$ ~ 1.61 Å and $r_{Ca^{2+}}$ ~ 1.34 Å) and Zr^{4+} ($r_{Zr^{4+}}$ ~ 1.45 Å) respective for the $(Bi_{0.5}Na_{0.5})^{2+}$ ($r_{Bi^{3+}}$ ~ 1.4Å and r_{Na^+} ~ 1.39 Å) and Ti^{4+} ($r_{Ti^{4+}}$ ~ 1.32 Å) sites in $(1-x)$BNKT–xBCTZ. The BNKT ceramic without the addition of BCTZ has a coexistence of rhombohedral and

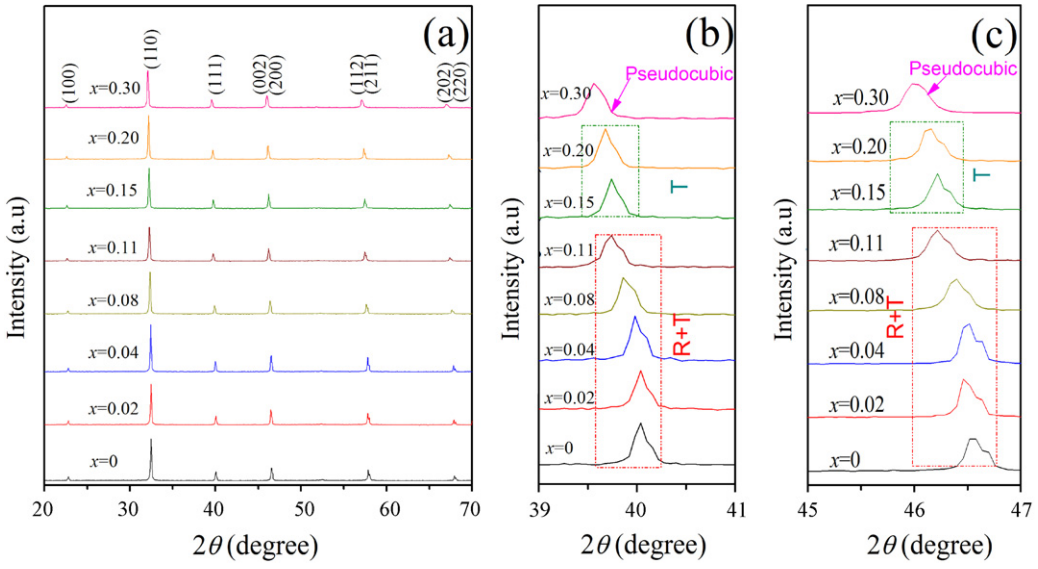

Fig. 1. (a) XRD patterns and (b) and (c) expanded XRD patterns of $(1-x)$BNKT–xBCTZ ceramics with different BCTZ contents.

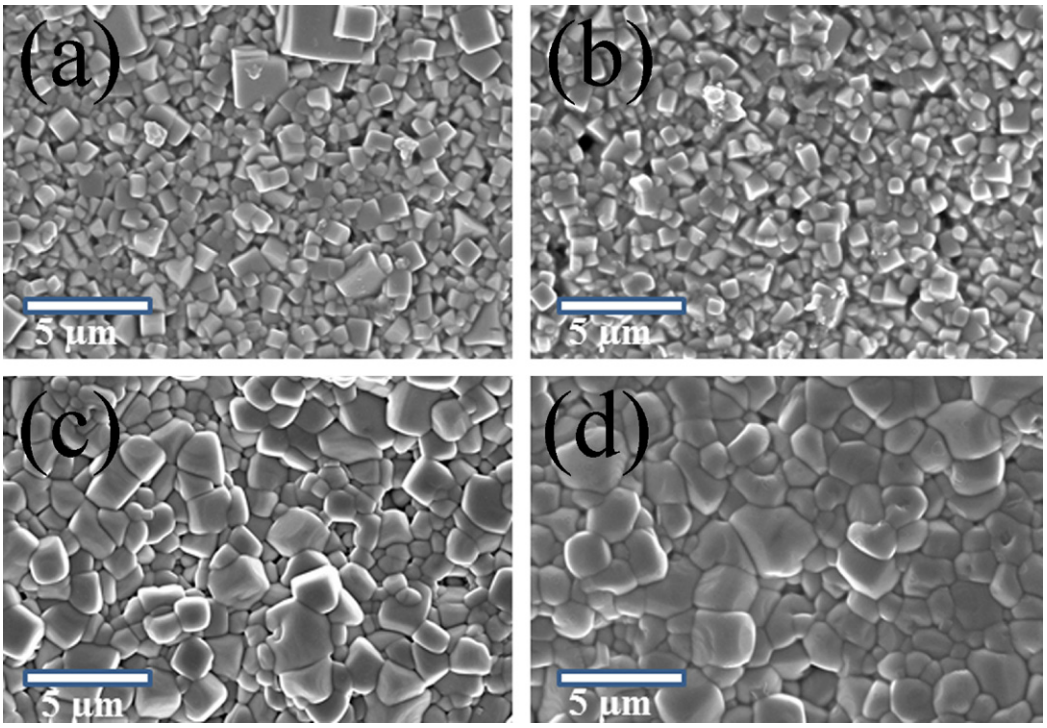

Fig. 2. SEM patterns of $(1-x)$BNKT–xBCTZ ceramics with different BCTZ contents: (a) $x = 0$, (b) $x = 0.02$, (c) $x = 0.15$, and (f) $x = 0.30$.

tetragonal phases as confirmed by the splitting of (0 0 2)/(2 0 0) peaks at $2\theta \sim 46^\circ$ and (1 1 1) peak at $2\theta \sim 40^\circ$. A coexistence of two phases is also maintained for these ceramics with $x < 0.15$, while a tetragonal phase is observed in these ceramics with $0.15 \leq x \leq 0.20$, as indicated by the splitting of (0 0 2)/(2 0 0) peaks at $2\theta \sim 46^\circ$ and a single (1 1 1) peak at $2\theta \sim 40^\circ$. However, the tetragonal distortion gradually diminished with increasing BCTZ content, and the split (0 0 2)/(2 0 0) peaks of the tetragonal phase finally merged into a single (2 0 0) peak at $x = 0.30$, suggesting that the crystal structure of these ceramics evolves from the tetragonal to a pseudocubic symmetry.

Fig. 2(a)–(d) shows the SEM patterns of $(1-x)$BNKT–xBCTZ ceramics with $x = 0$, 0.02, 0.15, 0.30, respectively. The dense microstructure is developed for all these ceramics in this work, regardless of BCTZ content. For pure BNKT ceramic, a mixture of small grains and large grains is observed, while a uniform grain is demonstrated for the ceramic with $x = 0.02$, as shown in Fig. 2(b). Moreover, it was observed that their grain

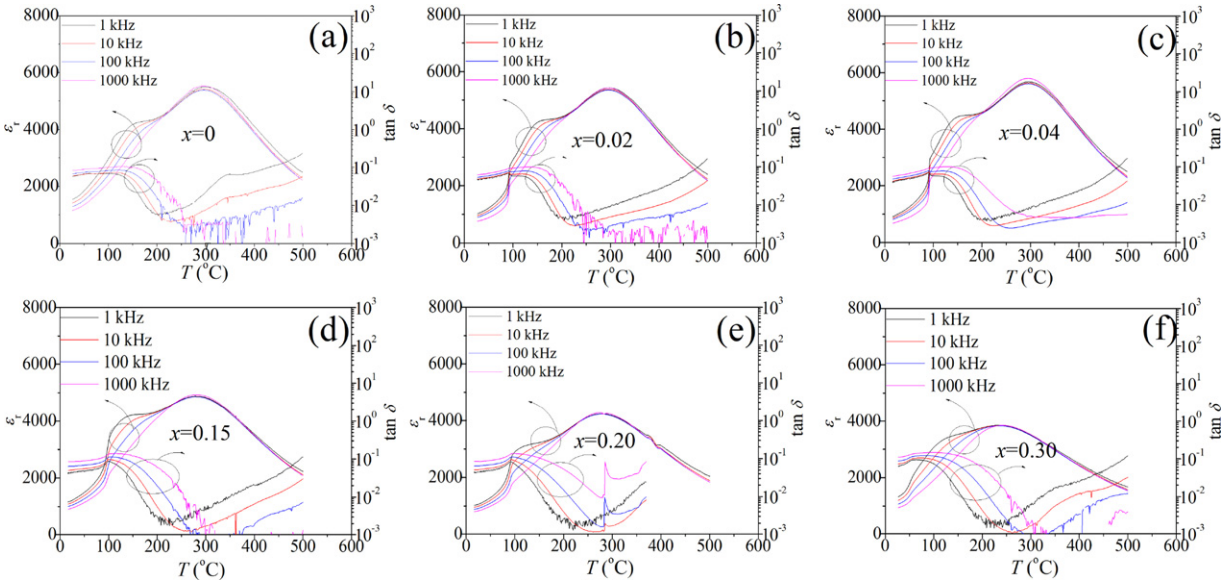

Fig. 3. Temperature dependent-dielectric properties of $(1-x)$BNKT–xBCTZ ceramics with different BCTZ contents: (a) $x = 0$, (b) $x = 0.02$, (c) $x = 0.04$, (d) $x = 0.15$, (e) $x = 0.20$, and (f) $x = 0.30$.

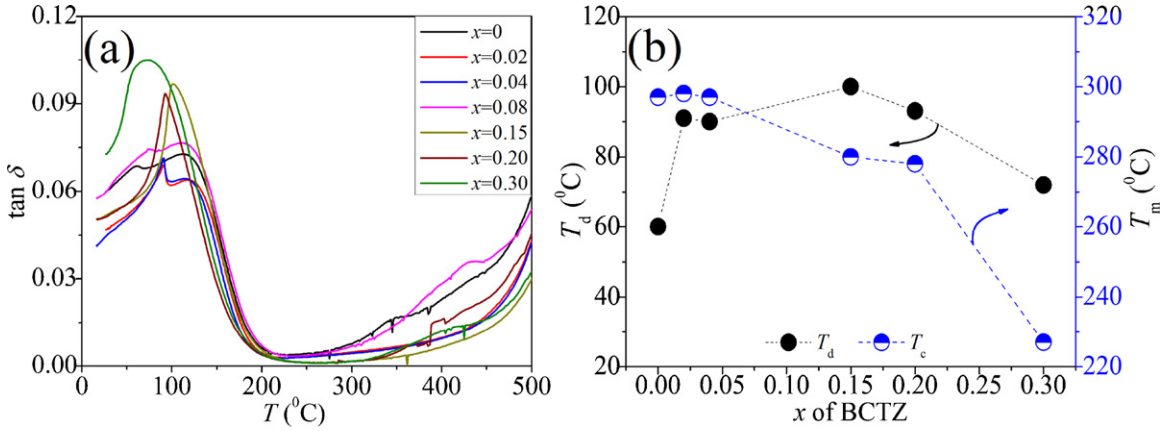

Fig. 4. (a) Temperature dependent-dielectric loss of (1−*x*)BNKT–*x*BCTZ ceramics with different BCTZ contents, and (b) T_m and T_d values as a function of BCTZ content.

sizes gradually increased with increasing BCTZ content, as shown in Figs. 2(a)–(d). Usually, the BCTZ ceramics need a high processing temperature, and the sintering temperature of (1−*x*)BNKT–*x*BCTZ ceramics increases with increasing BCTZ content. Therefore, an increase in grain sizes should be attributed to a higher sintering temperature of (1−*x*)BNKT–*x*BCTZ ceramics in this work.

Fig. 3 indicates the temperature dependence of the dielectric properties of (1−*x*)BNKT–*x*BCTZ ceramics, measured at 1, 10, 100, and 1000 kHz. As shown in Fig. 3, all the ceramics have two phase transitions located at T_d and T_m, where the T_d is defined as the depolarization temperature corresponding to the phase transition from a ferroelectric state to the "antiferroelectric" state, and the T_m is the maximum temperature at which the ε_r gets a maximum value corresponding to a phase transition from an "antiferroelectric" state to a paraelectric state [16]. However, the introduction of BCTZ results in an obvious difference of temperature versus dielectric properties, that is, the curve of these ceramics becomes more flatter with increasing BCTZ content. Broadened ε_r peaking at T_m suggests that these (1−*x*)BNKT–*x*BCTZ ceramics belong to relaxor ferroelectrics. For (1−*x*)BNKT–*x*BCTZ, A site (Na^+, Bi^{3+}, K^+, Ba^{2+}, Ca^{2+}) and B site (Ti^{4+}, Nb^{5+}, Zr^{4+}) are randomly distributed in the 12-fold coordination site and the 6-fold coordination site, respectively [17–20]. Therefore, the observed relaxor behavior could be attributed to the disordering of the A-site and B-site cations and the compositional fluctuation in the present work.

In this work, the temperature dependence of the dielectric loss (tan δ) has been used to determine the T_d value of (1−*x*)BNKT–*x*BCTZ ceramics [21]. Fig. 4(a) plots the temperature-dependent tan δ value of these (1−*x*)BNKT–*x*BCTZ ceramics, measured at 10 kHz. A tan δ peak is demonstrated in all the ceramics, confirming an involvement of a T_d into these ceramics above room temperature. Fig. 4(b) plots the T_d and T_m values of these ceramics. Their T_m value slightly decreases with increasing BCTZ content of $x \leq 0.20$, and then dramatically decreases with further increasing BCTZ content of $x > 0.20$. Moreover, the temperature for the first phase transition gradually shifts to a higher temperature with the addition of BCTZ ($x \leq 0.15$), and then decreases with further increasing BCTZ content of $x > 0.15$. Therefore, the introduction of an optimum BCTZ content contributes to the improvement of the T_d value of BNKT ceramics in this work, which is beneficial to the practical application of BNT-based ceramics.

Fig. 5 plots the d_{33} and k_p values of (1−*x*)BNKT–*x*BCTZ ceramics as a function of BCTZ content. Their d_{33} and k_p values increase with a small addition of BCTZ, reach a maximum value of $d_{33} \sim 143$ pC/N and $k_p \sim 0.29$ at $x = 0.02$, and then slowly decrease with further increasing BCTZ content. In this work, the enhanced piezoelectric properties should be attributed to the involvement of MPB in 0.98BNKT-0.02BCTZ ceramics. However, its d_{33} value is less than those of BNT-based ceramics reported by other authors [22–24]. Therefore, it is necessary to further improve the piezoelectric properties of 0.98BNKT-0.02BCTZ ceramics by some methods. In this work, we tried to improve the piezoelectric properties of 0.98BNKT–0.02BCTZ ceramics by optimizing sintering temperature and poling condition, and detailed descriptions were shown below.

It is well known that the sintering temperature plays an important role on the microstructure and electrical properties of piezoelectric ceramics [24–26], and thus it may be an effective way to improve the piezoelectric properties of these ceramics

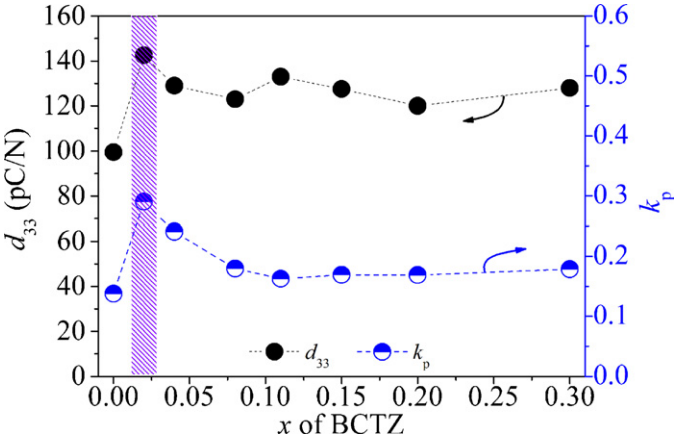

Fig. 5. Piezoelectric properties of (1−*x*)BNKT–*x*BCTZ ceramics with different BCTZ contents.

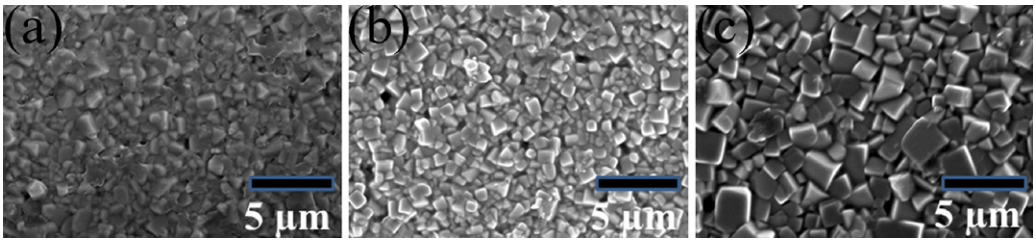

Fig. 6. SEM patterns of $(1-x)$BNKT–xBCTZ ceramics with $x = 0.02$ as a function of different sintering temperatures: (a) 1120 °C, (b) 1140 °C, and (c) 1180 °C.

with $x = 0.02$ by optimizing the sintering temperature. In this work, these ceramics with $x = 0.02$ were sintered at different temperatures of 1120–1200 °C in air in order to further improve their piezoelectric properties. Fig. 6 shows the SEM patterns of $(1-x)$BNKT–xBCTZ ceramics with $x = 0.02$ with different sintering temperatures. Its grain size dramatically becomes much larger when sintered at 1180 °C compared with that shown in SEM patterns in Figs. 6(a) and (b). Moreover, it was observed that some pores were demonstrated in these ceramics sintered at a low sintering temperature of ~1120 and ~1140 °C, and a denser microstructure is developed in the ceramic sintered at 1180 °C. Moreover, these ceramics sintered at 1180 °C have a higher density of ~5.89 g/cm^3 than that (~5.76 g/cm^3) of these ceramics sintered at 1140 °C. Subsequently, the influence of the poling electric field (E_p) on the d_{33} value was studied. Fig. 7 shows the dependence of the E_p on the d_{33} and Q_m values of these ceramics with $x = 0.02$ sintered at 1180 °C. The E_p significantly affects its d_{33} value. The d_{33} value is close to zero at $E_p \leq$ ~1.7 kV/mm due to the incomplete switching of the domain at $E_p < E_c$, and gradually increases with increasing E_p value because of the complete switching of the domain at $E_p > E_c$. The domain switching and rotation could be induced in 0.98BNKT–0.02BCTZ ceramics by raising the poling electric field, and then a better piezoelectric behavior is involved. In a low electric field, an 180° domain can be easily switched, while the 90°, 120°, 180° domains are also switched at a higher poling electric field [21]. A threshold field is ~1.7 kV/mm (~E_c) for the 0.98BNKT–0.02BCTZ ceramic in this work, which is much lower than those of BNT-based ceramics [22].

Fig. 8 plots the d_{33} and k_p values of $(1-x)$BNKT–xBCTZ ceramics as a function of different temperatures. A highest k_p value of ~0.34 is demonstrated in the ceramic sintered at 1160 °C, while the ceramic sintered at 1180 °C exhibits the largest d_{33} value of ~205 pC/N. Therefore, the ceramic sintered at 1180 °C has an optimum piezoelectric behavior of $d_{33} \sim 205$ pC/N and $k_p \sim 0.25$ because of a denser microstructure and a larger grain size by applying an optimum E_p value in this work.

Fig. 9(a) shows the polarization hysteresis loops (P–E) of $(1-x)$BNKT–xBCTZ ceramics with different BCTZ contents, measured at room temperature and 100 Hz. The P–E loop of these ceramics with $x = 0.02$ exhibits typical ferroelectric behavior, together with a larger remnant polarization (P_r) of ~28.1 μC/cm^2. Enhanced ferroelectric properties could be attributed to the involvement of MPB in the ceramic with $x = 0.02$. Fig. 9(b) shows the P–E loops of the ceramic with $x = 0.02$ sintered at different temperatures. Its P_r value gradually increases with increasing BCTZ content to $x = 0.02$, gets maximum value of ~31.8 μC/cm^2 when sintered at 1180 °C, and then decreases with increasing BCTZ content. Moreover, a lowest E_c value of ~19.1 kV/cm is induced for these ceramics sintered at 1180 °C because of the increased grain size and reduced grain boundaries. Therefore, an optimum sintering temperature contributes to the improvement of the ferroelectric properties of 0.98BNKT–0.02BCTZ

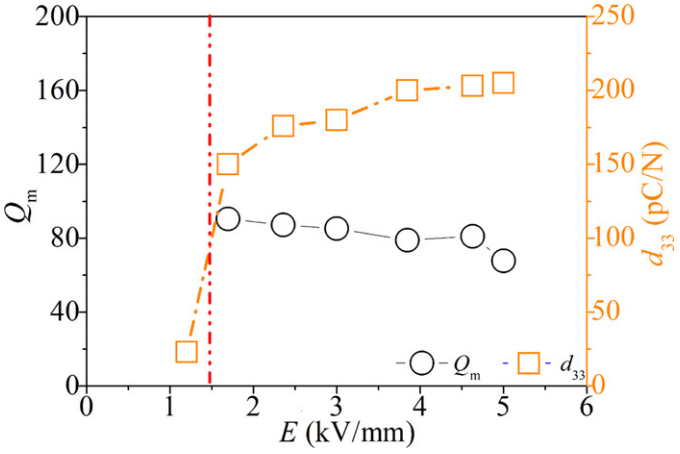

Fig. 7. d_{33} and Q_m values of $(1-x)$BNKT–xBCTZ ceramics with $x = 0.02$ as a function of applied electric field.

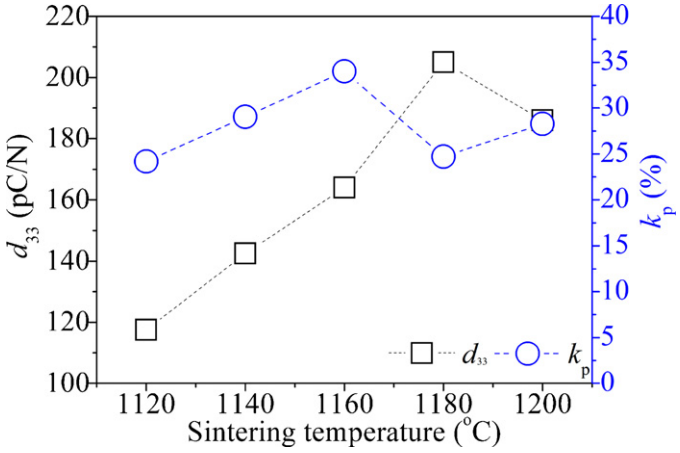

Fig. 8. Piezoelectric properties of $(1-x)$BNKT–xBCTZ ceramics sintered at different temperatures.

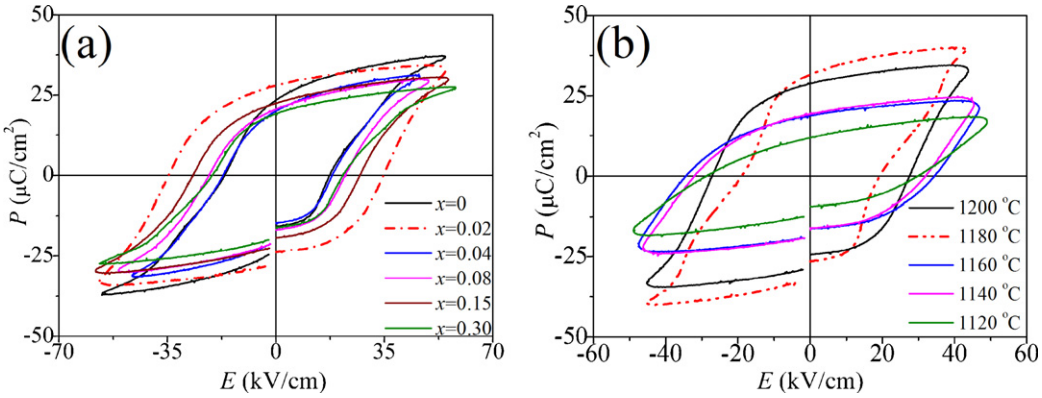

Fig. 9. *P–E* loops of (1−*x*)BNKT–*x*BCTZ ceramics (a) with different BCTZ contents and (b) sintered at different temperatures.

ceramics because of the higher density and the larger grain size in this work.

4. Conclusions

Lead-free $(1-x)Bi_{0.51}(Na_{0.82}K_{0.18})_{0.50}TiO_3$–$xBa_{0.85}Ca_{0.15}Ti_{0.90}Zr_{0.10}O_3$ ceramics were prepared by the conventional solid-state method. A stable solid solution is formed between BNKT and BCTZ, and a pure perovskite phase is demonstrated in all these ceramics. Their T_m and T_d value is strongly independent on the BCTZ content. Moreover, the sintering temperature and the poling electric field strongly affect the piezoelectric properties of the ceramic with $x = 0.02$. An optimum electrical behavior of $d_{33} \sim 205$ and $k_p \sim 0.25$ is demonstrated in the ceramic with $x = 0.02$ when sintered at 1180 °C and poled at an optimum electric field. As a result, the (1−*x*)BNKT–*x*BCTZ ceramic is a promising candidate material among lead-free piezoelectric ceramics.

Acknowledgments

This work was supported by the introduction of the National Natural Science Foundation of China (51102173), the introduction of talent start funds of Sichuan University (2082204144033), and the National University of Singapore.

References

[1] B. Jaff, W.R. Cook, H. Jaffe, Piezoelectric Ceramics, Academics Press, New York, 1971, pp. 115–181.
[2] T.R. Shrout, S.T. Zhang, Lead-free piezoelectric ceramics: alternatives for PZT? J. Electroceram. 19 (2007) 111–124.
[3] T. Takenaka, H. Nagata, Current status and prospects of lead-free piezoelectric ceramics, J. Eur. Ceram. Soc. 25 (2005) 2693–2700.
[4] J. Rödel, W. Jo, K.T.P. Seifert, E.M. Anton, T. Granzow, D. Damjanovic, Perspective on the development of lead-free piezoceramics, J. Am. Ceram. Soc. 92 (2009) 1153–1177.
[5] T. Takenaka, H. Nagata, Y. Hiruma, Phase transition temperatures and piezoelectric properties of $(Bi_{1/2}Na_{1/2})TiO_3$-and $(Bi_{1/2}K_{1/2})TiO_3$-based bismuth perovskite lead-free ferroelectric ceramics, IEEE Trans. Ultrason. Ferroelectr. Freq. Control 56 (2009) 1595–1612.
[6] F. Yan, S. Miao, I. Sterianou, I.M. Reaney, M.O. Lai, L. Lu, W.D. Song, Multiferroic properties and temperature-dependent leakage mechanism of Sc-substituted bismuth ferrite–lead titanate thin films, Scr. Mater. 64 (2011) 458–461.
[7] F. Yan, M.O. Lai, L. Lu, T.J. Zhu, Enhanced multiferroic properties and valence effect of Ru-doped $BiFeO_3$ thin films, J. Phys. Chem. C 114 (2010) 6994–6998.
[8] G.A. Smolenskii, V.A. Isupv, A.I. Agranovskaya, N.N. Krainik, The ferroelectric properties of strontium–bismuth titanate, Sov. Phys. Solid State 2 (1961) 2584–2594.
[9] Y.M. Li, W. Chen, Dielectric and ferroelectric properties of lead-free $Na_{0.5}Bi_{0.5}TiO_3$–$K_{0.5}Bi_{0.5}TiO_3$ferroelectric ceramics, Ceram. Int. 31 (2005) 139–142.
[10] A. Sasaki, T., Chiba, Y. Mamiya, E. Otsuki, Dielectric and piezoelectric properties of $(Bi_{0.5}Na_{0.5})TiO_3$–$(Bi_{0.5}K_{0.5})TiO_3$ systems, Jpn. J. Appl. Phys. Part 1 38 (1999) 5564–5567.
[11] X.X. Wang, X.G. Tang, H.L.W. Chan, Electromechanical and ferroelectric properties of $(Bi_{1/2}Na_{1/2})TiO_3$–$(Bi_{1/2}K_{1/2})TiO_3$–$BaTiO_3$ lead-free piezoelectric ceramics, Appl. Phys. Lett. 85 (2004) 91–93.
[12] W.F. Liu, X.B. Ren, Large piezoelectric effect in Pb-free ceramics, Phys. Rev. Lett. 103 (2009) 257602.
[13] D. Damjanovic, A morphotropic phase boundary system based on polarization rotation and polarization extension, Appl. Phys. Lett. 97 (2010) 062906.
[14] J.G. Wu, D.Q. Xiao, W.J. Wu, Q. Chen, J.G. Zhu, Composition and poling condition-induced electrical behavior of $(Ba_{0.85}Ca_{0.15})(Ti_{1-x}Zr_x)O_3$ lead-free piezoelectric ceramics, J. Eur. Ceram. Soc. 32 (4) (2012) 891–898.
[15] Y.S. Sung, J.M. Kim, J.H. Cho, T.K. Song, M.H. Kim, H.H. Chong, T.G. Park, D. Do, S.S. Kim, Effects of Na nonstoichiometry in $(Bi_{0.5}Na_{0.5+x})$-TiO_3 ceramics, Appl. Phys. Lett. 96 (2010) 022901.
[16] D.M. Lin, K.W. Kwok, H.L.W. Chan, Structure and electrical properties of $Bi_{0.5}Na_{0.5}TiO_3$–$BaTiO_3$–$Bi_{0.5}Li_{0.5}TiO_3$ lead-free piezoelectric ceramics, Solid State Ionics 178 (2008) 1930–1937.
[17] C. Karthik, N. Ravishankar, K.B.R. Varma, Relaxor behavior of $K_{0.5}La_{0.5}Bi_2Nb_2O_9$ ceramics, Appl. Phys. Lett. 89 (2006) 042905.
[18] Y. Hiruma, R. Aoyagi, H. Nagata, T. Takenaka, Ferroelectric and piezoelectric properties of $(Bi_{1/2}K_{1/2})TiO_3$ ceramics, Jpn. J. Appl. Phys. 44 (2005) 5040–5044.
[19] N. Setter, L.E. Cross, The role of B-site cation disorder in diffusion phase transition behavior of perovskite ferroelectrics, J. Appl. Phys. 51 (1980) 4356–4360.
[20] Y. Guo, K. Kakimoto, H. Ohsato, Dielectric and piezoelectric properties of lead-free $(Na_{0.5}K_{0.5})NbO_3$–$SrTiO_3$ ceramics, Solid State Commun. 129 (2004) 279–284.
[21] E.M. Anton, W. Jo, D. Damjanovic, J. Rödel, Determination of depolarization temperature of $(Bi_{1/2}Na_{1/2})TiO_3$-based lead-free piezoceramics, J. Appl. Phys. 110 (2011) 094108.
[22] D. Lin, D. Xiao, J. Zhu, P. Yu, Piezoelectric and ferroelectric properties of $[Bi_{0.5}(Na_{1-x-y}K_xLi_y)_{0.5}]TiO_3$ lead-free piezoelectric ceramics, Appl. Phys. Lett. 88 (2006) 062901.

[23] D.M. Lin, D.Q. Xiao, J.G. Zhu, P. Yu, H.J. Yan, L.Z. Li, Synthesis and piezoelectric properties of lead-free piezoelectric [$Bi_{0.5}(Na_{1-x-y}K_xLi_y)_{0.5}$] TiO_3 ceramics, Mater. Lett. 58 (2004) 615–618.

[24] C. Xu, D. Lin, K.W. Kwok, Structure, electrical properties and depolarization temperature of $(Bi_{0.5}Na_{0.5})TiO_3$–$BaTiO_3$ lead-free piezoelectric ceramics, Solid State Sci. 10 (2008) 934–940.

[25] A.A. Cavalheiro, J.C. Bruno, M.A. Zaghete, J.A. Varela, Effect of lithium additive on the microstructure and electrical responses of 0.9PMN–0.1PT ceramics, J. Mater. Sci. 42 (2007) 828.

[26] R. Hong, F. Gao, J. Liu, Y. Yao, C. Tian, Fabrication of $(Bi, Na)_{0.5}TiO_3$–$BaTiO_3$ textured ceramics by tape casting, J. Mater. Sci. 43 (2008) 6126–6131.